

RAVEL: Rare Concept Generation and Editing via Graph-driven Relational Guidance

Kavana Venkatesh¹ Yusuf Dalva¹ Ismini Lourentzou² Pinar Yanardag¹
¹Virginia Tech ²UIUC
 {kavanav,ydalva,pinary}@vt.edu {lourent2}@illinois.edu
<https://ravel-diffusion.github.io>



Figure 1. We introduce RAVEL, a training-free approach that uses graph-based RAG to enhance T2I models with context-aware guidance. It improves generation of rare, complex concepts and supports disentangled image editing. A self-correction module further refines visual and narrative accuracy.

Abstract

Despite impressive visual fidelity, current text-to-image (T2I) diffusion models struggle to depict rare, complex, or culturally nuanced concepts due to training data limitations. We introduce RAVEL, a training-free framework that significantly improves rare concept generation, context-driven image editing, and self-correction by integrating graph-based retrieval-augmented generation (RAG) into diffusion pipelines. Unlike prior RAG and LLM-enhanced methods reliant on visual exemplars, static captions or pre-trained knowledge of models, RAVEL leverages structured knowledge graphs to retrieve compositional, symbolic, and relational context, enabling nuanced grounding even in the absence of visual priors. To further refine generation quality, we propose SRD, a novel self-correction module that iteratively updates prompts via multi-aspect alignment feedback, enhancing attribute accuracy, narrative coherence, and semantic fidelity. Our framework is model-agnostic and compatible with leading diffusion models including Stable Diffusion XL, Flux, and DALL-E 3. We conduct extensive evaluations across three newly proposed benchmarks - MythoBench, Rare-Concept-1K, and NovelBench. RAVEL also consistently outperforms SOTA methods across perceptual, alignment, and LLM-as-a-Judge metrics. These results position RAVEL as a robust paradigm for controllable and

interpretable T2I generation in long-tail domains.

1. Introduction

Recent advances in T2I diffusion models [20, 30, 33, 35, 40] have led to striking progress in generating visually rich imagery from natural language prompts. However, these models remain inherently limited by the scope and distribution of their training data, which tends to underrepresent rare, complex, or culturally nuanced concepts [49]. As a result, T2I models often fail to accurately depict entities or scenarios that fall outside common visual domains, ranging from real-world long-tail concepts like a ‘unicycle’ or ‘Boston bull’ to intricate historical figures, symbolic relationships, and imaginative fictional constructs [36]. This highlights a critical bottleneck in the generalizability and contextual grounding of current generative models when faced with sparsely represented or visually undocumented concepts.

To overcome these limitations, users often resort to writing highly detailed prompts to guide the models toward the desired outputs [25, 45, 47]. However, this process is time-consuming and requires extensive manual trial-and-error, domain expertise, as well as understanding of the model’s specific vocabulary and biases. Another approach is to fine-tune models on specialized datasets, typically by training

new low-rank adaptations (LoRAs) [21] or creating custom embeddings [14] for each unique concept. Although effective, these methods require significant computational resources, time, and technical expertise, making them costly and impractical for users without advanced skills. Recent approaches like prompt engineering, adapter modules, and few-shot learning have aimed to extend model capabilities without full-scale retraining [1, 50, 54], yet they depend heavily on extensive user input and still work within the boundaries of the model’s existing knowledge. Fine-tuning LLMs on domain-specific data for contextual guidance is resource intensive, prone to issues like hallucination and catastrophic forgetting [13], and often struggles to capture fine-grained and relational details accurately [16].

Retrieval-Augmented Generation (RAG) [23] techniques have been introduced to expand context in large language models (LLMs) [42], leveraging external knowledge to improve generation consistency and depth. Prior RAG-based methods [1, 3, 6, 18, 27, 28, 38, 39, 41] augment generation using retrieved image-text pairs, captioned concepts, or diffusion trajectories from large-scale databases. While effective for reference-based style transfer, these approaches (1) assume the existence of visually similar examples, (2) lack fine-grained or relational reasoning, and (3) operate in a single-pass, non-iterative fashion. In contrast, **our method is the first to use structured knowledge graphs as the retrieval backbone**, enabling symbolic, relational, and factual grounding without requiring visual exemplars. Moreover, our novel SRD module introduces an iterative self-correction loop that dynamically identifies missing attributes and issues targeted refinements, which is absent in all prior RAG-T2I methods.

To address these limitations, we propose a novel framework that augments T2I diffusion models with a graph-based RAG system. Our approach dynamically retrieves structured textual context from a knowledge graph, enabling diffusion models to generate semantically rich, contextually grounded images, even for rare or unseen concepts beyond their training data. This integration enhances not only the accuracy and consistency of generations, but also their interpretability and cultural fidelity without requiring additional user input or fine-tuning. The framework is model-agnostic and compatible with popular diffusion systems, including Flux [10], Stable Diffusion [34], DALL·E [31], and ControlNet [52]. Beyond generation, it also improves image editing within ControlNet by injecting contextual cues into the editing prompt, enabling finer control and semantic precision. Additionally, we introduce a self-correction mechanism (SRD) that iteratively refines outputs based on vision-language alignment across key dimensions such as appearance, narrative coherence, and cultural relevance. Unlike prior self-correcting methods [48, 56] that rely on the static internal knowledge of pretrained LLMs, our RAG-driven

loop dynamically expands the contextual window, allowing for structured, multi-aspect refinement. This leads to significantly improved fidelity and semantic alignment, pushing the boundaries of interpretable and controllable generative modeling. Our contributions are as follows:

- We propose RAVEL, a framework that augments text-to-image diffusion models by dynamically retrieving relevant information from a structured knowledge graph to generate complex rare concepts across diverse domains. To our knowledge, RAVEL represents the first instance of leveraging Knowledge Graph-Based RAG to improve both image generation and image editing.
- We propose a novel RAG context-driven self-correction approach for image generation, refining outputs iteratively by using structured knowledge to address inaccuracies, achieving coherence in complex visual narratives.
- We release three new benchmarks - *MythoBench*, *Rare-Concept-1K*, and *NovelBench*, designed to rigorously evaluate generative models on cultural symbolism, fine-grained attribute grounding, and long-tail generalization. These resources provide the first comprehensive testbeds for rare concept generation and editing under structured, multi-aspect evaluation.

2. Related Work

Large Language Models and RAG Large Language Models (LLM) have shown remarkable human-like general text generation abilities for a variety of tasks [5, 31], further enhanced by prompt engineering [5, 7, 43, 46, 51]. Retrieval Augmented Generation (RAG) [23] is a prompt engineering technique that improves the relevance and accuracy of a generative model’s response, while reducing hallucinations [2]. Knowledge Graphs (KG) consist of consistent nodes and relationships to store information in a structured way. KGs are extensively being used as databases for RAG frameworks [32, 37] due to their scalability, interpretability and extendability. In our work, we leverage KGs to store structured and rich contextual data to enhance T2I diffusion model prompts.

LLMs and RAG for T2I Diffusion Models Advancements in large language models (LLMs) have enhanced text-to-image (T2I) diffusion models, improving image fidelity and prompt alignment. Recent approaches have leveraged LLMs to generate layouts with bounding boxes for better spatial organization in complex, multi-object scenes [11, 12, 15, 24]. Prompt engineering also extends T2I models’ narrative understanding [54], while fine-tuning LLMs on high-quality prompts improves output [50] but can be costly and less adaptable, with risks of forgetting and hallucination. Retrieval-augmented generation (RAG) [23] further enhances T2I models by retrieving relevant images or prompts from vector databases, aiding in style and concept alignment [1, 3, 6, 18, 27, 28, 38, 39, 41]. How-

ever, these approaches remain constrained by their reliance on retrieved visual exemplars and single-pass pipelines. They lack the ability to reason over fine-grained, structured knowledge, making them less effective for rare concept generation, context fidelity, and self-correcting edits, capabilities central to our proposed method. LLM-controlled methods in image editing, like DiffEdit [8] for targeted edits and Hive [53] for compositional edits, show promise but struggle with domain consistency. Techniques such as Instruct-Pix2Pix [4] and Prompt2Prompt [19] facilitate global edits but lack precision in finer details, highlighting the limitations in meeting nuanced, context-sensitive editing needs.

3. Method

3.1. Knowledge Graph Construction

We employ a knowledge graph-based RAG framework to enhance T2I models to generate rare concepts beyond their pretraining distribution, without relying on visual priors. Unlike unstructured retrieval, knowledge graphs encode entities, attributes, and relationships explicitly, enabling precise, compositional, and interpretable context. Our domain-agnostic graph construction follows a two-phase automated pipeline. Given a domain template, we scrape high-quality data (e.g., Wikipedia, verified sources) and apply Chain-of-Thought [46] reasoning and Few-Shot prompting [5] to extract structured, attribute-rich descriptions - e.g., taxonomy and habitat for species, or appearance and symbolic artifacts for cultural figures. In phase one, we create per-entity graphs using LLM-generated graph queries; in phase two, we form bidirectional links to support relational reasoning (e.g., associating hummingbirds via pollination traits or referencing historical events). This modular pipeline generalizes across domains by adapting data sources and attribute schemas.

3.1.1. Graph-Based RAG

Consider a simple user prompt \mathcal{P} such as “red ginger blooming in a garden”. Our approach first leverages an LLM to identify core entities and related concepts; e.g., botanical species, scene setting, and potential relational cues. Once key entities are extracted, we employ an LLM to dynamically generate graph queries to retrieve their associated attributes and relationships from the knowledge graph. This yields a structured context set that encompasses both appearance features (e.g., bract shape, color, arrangement) and relational cues (e.g., pollinator = hummingbird, habitat = tropical forests). The retrieved context is then expanded using Contrastive CoT prompting [7] to highlight multiple visual and narrative dimensions, creating a richly grounded prompt that would be tedious to manually author.

Image Generation: Given a high-level user prompt \mathcal{P} , we generate a context-enriched prompt \mathcal{P}' by leveraging knowledge graph-based RAG and feed it to the T2I model.

By enriching the initial prompts with extensive contextual and appearance information, RAVEL enables the generation of accurate visual representations.

Image Editing: Given an input image and an editing prompt \mathcal{P}_e such as “Add the pollinator of red ginger”, RAVEL queries the knowledge graph to retrieve precise contextual details; e.g., pollinators like hummingbird, orchid bee, or butterfly. This ensures the accurate and semantically grounded addition of the correct entity to the image, in contrast to standard ControlNet, which may insert a generic or unrelated object due to the lack of symbolic guidance.

3.2. Self-Correcting RAG-Guided Diffusion (SRD)

While our graph-augmented generation significantly improves accuracy, complex rare concepts with fine-grained attributes may still contain errors or omissions. To address this, we introduce **Self-Correcting RAG-Guided Diffusion (SRD)**, an iterative refinement mechanism that progressively corrects these issues by analyzing generated images and updating prompts based on graph context.

Initialization and Setup. Given the initial zero-shot image I_0 , generated from the enhanced prompt P_0 (Section 3.1.1), SRD compares I_0 to target features T , derived from the RAG context to identify misalignments. We define two alignment metrics: a per-feature *Stability Score* $s_i \in [0, 1]$ indicating correctness of feature i , and the *Global Stability Index*, GSI , which averages scores across all features. SRD is triggered when $GSI(I_0) < GSI_\epsilon$. To refine the image, SRD iteratively adjusts prompts using RAG context guidance. A decay factor d , (starting at 0.9, decreasing each round) scales prompt adjustments at each iteration k , preventing overcorrection while allowing aggressive early fixes. A *Change Tracking Matrix*, S_{tracker} records stability counts for each feature across K iterations. Features stable for N consecutive rounds are ‘locked’ to prevent regression. The process terminates when $GSI \geq GSI_\epsilon$, or when iteration limit K is reached.

Iterative Refinement and Stability Tracking. The SRD loop executes for up to K iterations, refining prompts and regenerating images to improve fidelity. At each step k , image I_k is generated from prompt P_{k-1} . An LLM analyzes I_k to assess current features F_{curr} , computing stability scores in S_{tracker} based on alignment with target features T . For instance, in the case of a red ginger plant, the system evaluates visual features such as bract structure, arrangement, and glossiness. If any attributes are missing, hallucinated, or regressing, the prompt is refined by adjusting contextual emphasis, modulated by a decay factor, d . If $F_{\text{curr}} = T$ and all feature scores meet the stability threshold $S_{\text{threshold}}$, the process halts early due to sufficient alignment. Through this iterative refinement, SRD adapts its prompt refinement process to each feature’s stability status, creating a feedback loop that converges on high fidelity without

excessive intervention.

4. Experiments

We evaluate RAVEL across a broad range of qualitative and quantitative experiments to assess its performance in rare concept generation, contextual editing, and iterative self-correction. Our framework is tested across three state-of-the-art text-to-image (T2I) models - such as Flux, Stable Diffusion XL (SDXL), and DALL-E 3.

Datasets and Domains: We conduct experiments across more than 15 diverse rare concept categories, including rare animals, birds, fashion elements, architectural artifacts, symbolic cultural figures, and complex mythological characters. Our dataset is curated from a wide range of validated sources, including Wikipedia, original mythological texts, and narrative-rich domains from Project Gutenberg. Each concept is enriched using structured, multi-attribute prompting from a knowledge graph, enabling context-aware generation across domains.

Benchmarks: We report performance on 100 relatively rare image prompts carefully chosen from the T2I-CompBench [22], an established benchmark that evaluates compositional and attribute-based accuracy in T2I generation. To address gaps in existing evaluation protocols and enable principled assessment of rare concept generation, we introduce **three novel benchmarks**, each designed to target a specific axis of rarity, generalization, and symbolic complexity:

- **MythoBench:** The first benchmark for mythological and culturally symbolic concepts, containing 500 character prompts across three difficulty tiers (simple, composite, relational) based on narrative depth & visual complexity.
- **Rare-Concept-1K:** A 1,000-prompt benchmark spanning five underrepresented categories - obsolete technologies, rare creatures, cultural artifacts, architectural objects, and uncommon tools. Each includes 200 manually verified concepts with structured contextual descriptions to evaluate attribute fidelity, domain-specific grounding.
- **NovelBench:** A zero-shot benchmark of 500 prompts sourced from Project Gutenberg (e.g., folklore, speculative fiction, period literature), designed to test generalization to unseen, narrative-rich, and archaic concepts under distribution shift.

These benchmarks address the lack of reliable ground-truth imagery in rare domains and support comprehensive evaluation across symbolic reasoning, real-world rarity, and narrative generalization. We use four LLM-as-a-Judge [55] metrics: Attribute Accuracy, Context Relevance, Visual Fidelity, and Intent Representation.

Experimental Setup: For data curation, we leverage Neo4j [29] as our knowledge graph database storing data of more

than 600 distinct rare concepts and utilize GPT-4o as our LLM for all tasks. Each prompt is enriched with additional context retrieved by our RAG framework using Contrastive CoT prompting for output rare image generation. To evaluate these generated outputs, we sample 500 prompts from the above four benchmarks and generate the 500 images each using three models—Stable Diffusion XL Base 1.0, Flux.1 [dev], and DALL-E 3, under both base prompt conditions (only name of a concept) and context-enhanced conditions across the 15+ categories. For image editing and self-correction, we assess our framework on 150 images featuring 38 distinct characters. To effectively capture fine-grained details, we set the guidance scale within a range of 15 to 30. GSI_ϵ is set to 23 for SRD. All experiments are conducted on a single NVIDIA L40 GPU. For evaluation, we employ a multi-faceted approach to assess both our RAG system and the generated images. Given the complexity of domain-specific fine-grained details, we adopt the LLM-as-a-Judge framework [55], implemented using G-Eval [26] from the open-source DeepEval [9] library across our four benchmarks to isolate category-based performance. Additionally, we compute traditional computer vision metrics to quantify image quality and alignment across concepts sampled from the four benchmarks as mentioned and compare RAVEL with several SOTA methods for rare image generation, relational editing and self-correction.

4.1. Qualitative Results

RAVEL also effectively generates complex global mythology and fictional concepts without prior visual exemplars.

Image Editing: Figure 3 demonstrates how RAVEL, when integrated with ControlNet, enables precise and context-aware image editing using relational cues. We compare edits on three types of entities - plants (*red ginger*), animals (*saluki*), and mythological characters (*Shiva*, *Jambavan*) under attribute-driven prompts (e.g., *+pollinator*, *+habitat*, *+daughter*). Without our method, ControlNet often fails to apply meaningful edits or resorts to generic insertions. In contrast, RAVEL accurately grounds edits in concept-specific relational knowledge, such as pairing Shiva with his snake companion *Vasuki* or placing red ginger in its tropical forest habitat, and adding hummingbird as its pollinator. Our method consistently adds narratively coherent, visually distinct, and semantically grounded elements without requiring explicit visual supervision.

Self-Correction for Image Alignment: Figure 4 illustrates how our SRD module incrementally improves image fidelity through iterative, context-aware prompt refinement. Starting from an initial generation (Flux + Ours), SRD analyzes visual deviations relative to the target attributes retrieved from the knowledge graph and refines the prompt over successive rounds (R1, R2). This allows SRD to correct both fine-grained structure and high-level semantics.

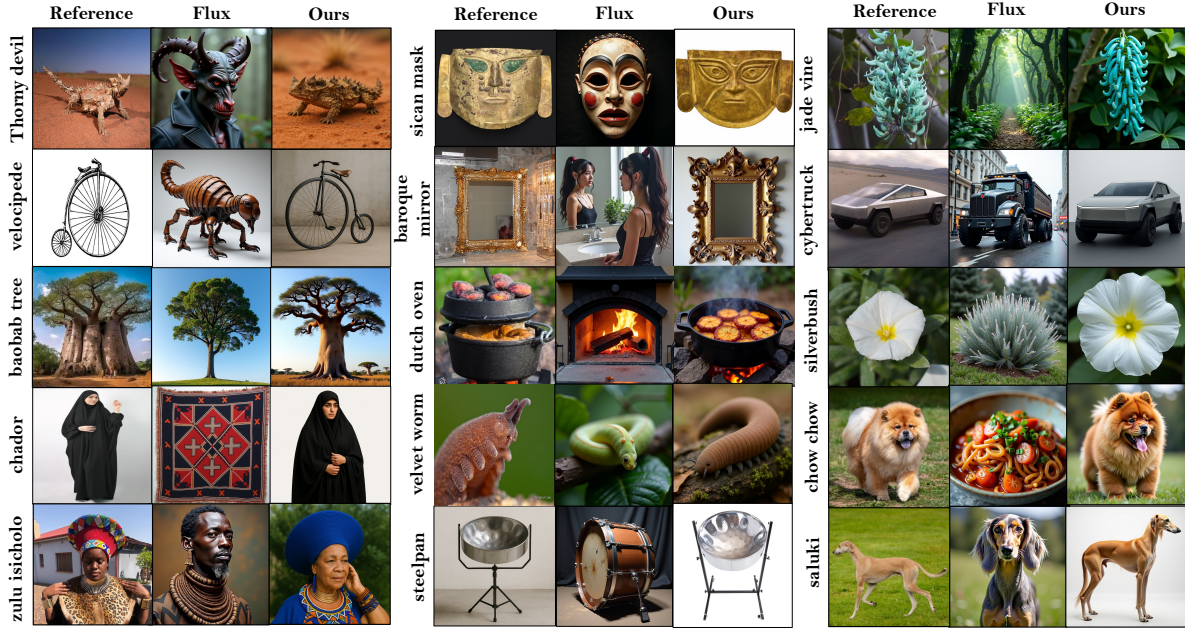


Figure 2. RAVEL enhances image generation by integrating contextual details often overlooked by standard models for a variety of domains. *Note that the reference images are shown solely for illustrative purposes and are not used by our framework.*

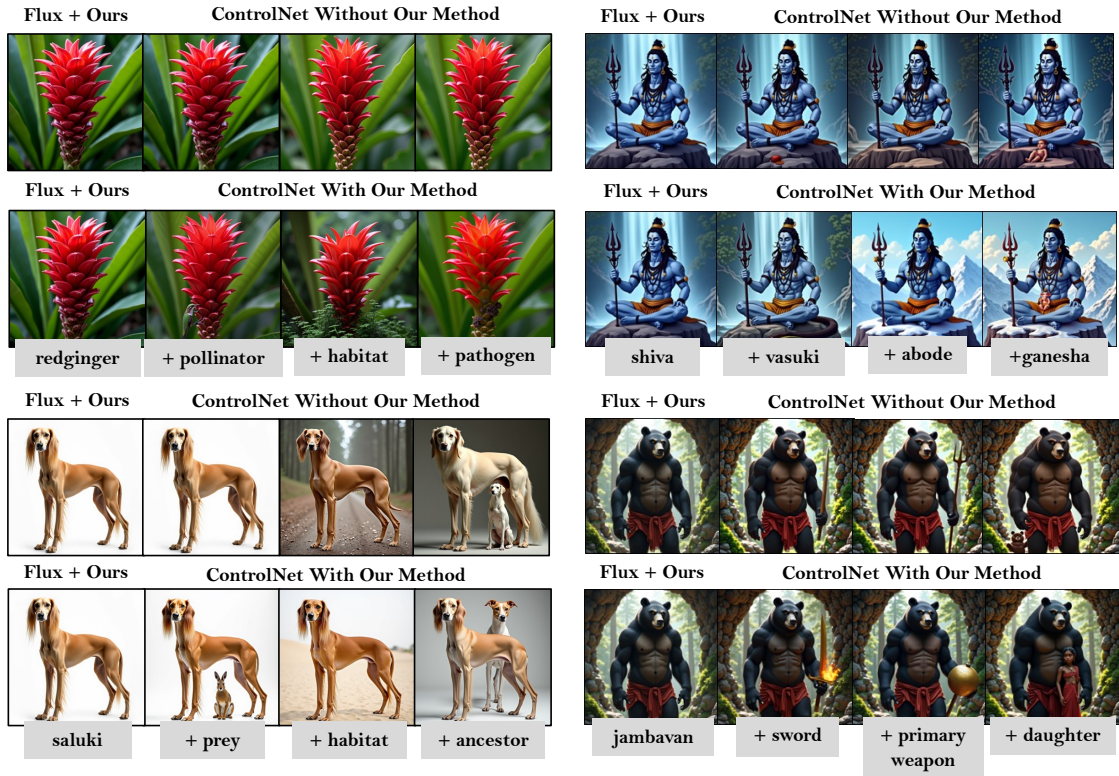


Figure 3. Our method enhances disentangled editing by adding relationally accurate elements without explicit instructions, while ControlNet either adds generic objects or fails to make any edit.

Table 1. LLM-as-a-Judge Evaluation Across Multiple Benchmarks. RAVEL significantly improves alignment, particularly on knowledge-intensive datasets. * Δ_{avg} (change in average performance).

Benchmark	Metric	SDXL	Flux	DALL-E3	SDXL+Ours	Flux+Ours	DALL-E+Ours	Δ_{avg}
T2I-CompBench [22]	Comp. Accuracy	0.5120 \pm 0.009	0.5870 \pm 0.007	0.6230 \pm 0.011	0.7210 \pm 0.012	0.7980 \pm 0.009	0.8320 \pm 0.012	+0.206
	CLIP-I	0.2730 \pm 0.010	0.3180 \pm 0.012	0.3510 \pm 0.011	0.6620 \pm 0.010	0.7010 \pm 0.011	0.7280 \pm 0.012	+0.189
	BLIP-VQA	0.2120 \pm 0.011	0.2510 \pm 0.010	0.2790 \pm 0.009	0.4240 \pm 0.010	0.4530 \pm 0.011	0.4680 \pm 0.010	+0.215
MythoBench	Attr. Accuracy	0.3470 \pm 0.011	0.4070 \pm 0.006	0.5000 \pm 0.008	0.7790 \pm 0.010	0.8650 \pm 0.013	0.8820 \pm 0.010	+0.456
	Context Relevance	0.4570 \pm 0.009	0.5530 \pm 0.007	0.5600 \pm 0.014	0.8490 \pm 0.011	0.8840 \pm 0.011	0.9240 \pm 0.014	+0.341
	Intent Repres.	0.3320 \pm 0.009	0.3160 \pm 0.010	0.5120 \pm 0.014	0.8090 \pm 0.012	0.8990 \pm 0.007	0.8540 \pm 0.014	+0.496
	Visual Fidelity	0.4190 \pm 0.010	0.5040 \pm 0.009	0.5390 \pm 0.010	0.7620 \pm 0.011	0.8120 \pm 0.010	0.8290 \pm 0.012	+0.304
	Overall Score	0.3888 \pm 0.023	0.4450 \pm 0.023	0.5278 \pm 0.018	0.7998 \pm 0.015	0.8650 \pm 0.017	0.8723 \pm 0.018	+0.393
Rare-Concept-1K	Attr. Accuracy	0.3980 \pm 0.010	0.4670 \pm 0.007	0.5230 \pm 0.010	0.7410 \pm 0.012	0.8120 \pm 0.009	0.8450 \pm 0.014	+0.348
	Context Relevance	0.4210 \pm 0.014	0.5010 \pm 0.007	0.5480 \pm 0.012	0.6980 \pm 0.010	0.7890 \pm 0.011	0.8210 \pm 0.014	+0.279
	Intent Repres.	0.3890 \pm 0.008	0.4450 \pm 0.014	0.5370 \pm 0.012	0.7120 \pm 0.010	0.8010 \pm 0.014	0.8340 \pm 0.009	+0.312
	Visual Fidelity	0.4350 \pm 0.009	0.5010 \pm 0.010	0.5340 \pm 0.011	0.7390 \pm 0.010	0.7940 \pm 0.009	0.8180 \pm 0.010	+0.290
	Overall Score	0.4108 \pm 0.019	0.4785 \pm 0.018	0.5355 \pm 0.017	0.7225 \pm 0.013	0.7990 \pm 0.015	0.8295 \pm 0.014	+0.309
NovelBench	Attr. Accuracy	0.4210 \pm 0.014	0.5120 \pm 0.010	0.5670 \pm 0.006	0.7650 \pm 0.007	0.8430 \pm 0.010	0.8780 \pm 0.010	+0.334
	Context Relevance	0.4480 \pm 0.006	0.5340 \pm 0.014	0.5890 \pm 0.014	0.8120 \pm 0.011	0.8710 \pm 0.009	0.9010 \pm 0.014	+0.319
	Intent Repres.	0.4120 \pm 0.013	0.4780 \pm 0.011	0.5430 \pm 0.007	0.7890 \pm 0.007	0.8560 \pm 0.012	0.8670 \pm 0.006	+0.382
	Visual Fidelity	0.4320 \pm 0.010	0.5070 \pm 0.009	0.5510 \pm 0.010	0.7580 \pm 0.010	0.8260 \pm 0.011	0.8510 \pm 0.009	+0.305
	Overall Score	0.4283 \pm 0.012	0.5078 \pm 0.015	0.5625 \pm 0.011	0.7810 \pm 0.006	0.8490 \pm 0.010	0.8740 \pm 0.013	+0.327

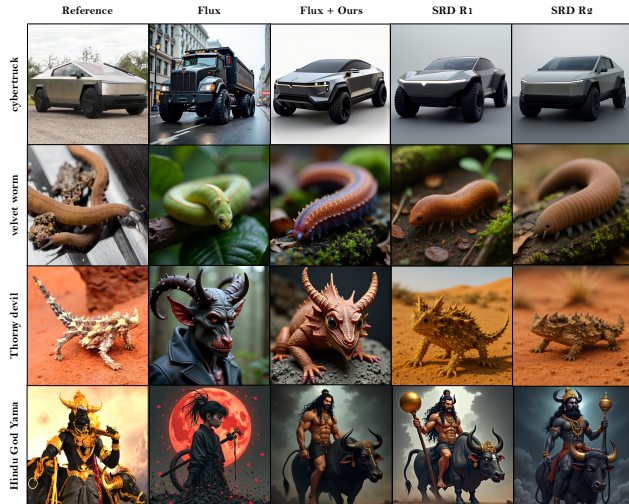


Figure 4. Our self-correction mechanism ensures accurate depictions of concepts via iterative, context-aware prompt refinement.

For example, SRD sharpens the geometric body contours of the *cybertruck*, fixes segmentation and texture inconsistencies in the *velvet worm*, restores accurate spines and proportions in the *thorny devil*, and adjusts appearance traits such as posture, accessories, and symbolic objects for *Yama*. Compared to prior self-editing approaches [48, 56], which depend solely on an LLM’s internal knowledge, SRD leverages retrieved, concept-specific context and thus produces more stable and interpretable corrections. The refinement process is model-agnostic and applies consistently across T2I architectures, including Flux, SDXL, and DALL-E.

4.2. Quantitative Results

We comprehensively evaluate RAVEL across three tasks: rare concept generation, knowledge-grounded editing, and iterative self-correction. To assess low-level alignment and perceptual quality, we report standard image-text metrics across all tasks and backbones (Flux, SDXL, DALL-E 3). See tables 2 and 3. For high-level semantic alignment, we benchmark on *T2I-CompBench* and three new datasets introduced in this work - *MythoBench*, *Rare-Concept-1K*, and *NovelBench*, each targeting rare or culturally grounded concepts with varying difficulty (see table 1). We evaluate these using our LLM-as-a-Judge framework with interpretability-aware metrics: *Attribute Accuracy Index (AAI)*, *Context Relevance Score (CRS)*, *Intent Representation Metric (IRM)*, and *Visual Fidelity Score (VFS)*, implemented via the GEval library [17].

4.3. T2I-CompBench Results

We compare RAVEL against state-of-the-art methods in RAG-based generation [3, 27, 36, 38], LLM-enhanced prompting [12, 15, 24], model-based editing [44, 53], and self-correction [48, 56]. Across all benchmarks, RAVEL demonstrates consistent gains in alignment, controllability, and fidelity, particularly for abstract, rare, and culturally nuanced concepts. Using G-Eval [26], we further evaluate our KG-RAG pipeline’s retrieval and generation quality through context relevance and answer accuracy metrics.

Table 2 shows the performance comparison of our approach across various text-image alignment, semantic coherence, and perceptual quality metrics against Flux, SDXL, and DALL-E 3 over a set of 500 images. Traditional models such as CLIP often struggle with fine-grained, domain-specific attributes of rare concepts, making direct

Table 2. **Performance on Rare Concept Generation.** Our method significantly improves text-image alignment and attribute accuracy across multiple diffusion backbones.

Method	CLIP-T \uparrow	CLIP-I \uparrow	DINO v2 \uparrow	BLIP-VQA \uparrow	LPIPS \downarrow	SigLIP \uparrow
Baseline Models						
Flux	0.1871 \pm 0.012	0.4178 \pm 0.025	0.2871 \pm 0.019	0.2778 \pm 0.018	0.5802 \pm 0.031	0.0634 \pm 0.007
SDXL	0.1842 \pm 0.013	0.2971 \pm 0.021	0.2619 \pm 0.017	0.1994 \pm 0.016	0.6234 \pm 0.034	0.0335 \pm 0.005
DALL-E	0.2201 \pm 0.014	0.4802 \pm 0.027	0.3667 \pm 0.022	0.2789 \pm 0.020	0.5677 \pm 0.030	0.0689 \pm 0.008
RAG-Based Methods						
ImageRAG [38]	0.2841 \pm 0.026	0.5175 \pm 0.011	0.2877 \pm 0.002	0.2162 \pm 0.0012	0.6538 \pm 0.030	0.0420 \pm 0.010
*RDM [3]	0.2985 \pm 0.021	0.5102 \pm 0.010	0.3017 \pm 0.010	0.2345 \pm 0.013	0.5908 \pm 0.0145	0.0485 \pm 0.012
ReCon [27]	0.2791 \pm 0.012	0.4986 \pm 0.031	0.2811 \pm 0.012	0.2215 \pm 0.013	0.6681 \pm 0.010	0.0376 \pm 0.020
SeedSelect [36]	0.1976 \pm 0.010	0.4801 \pm 0.021	0.2789 \pm 0.011	0.2013 \pm 0.032	0.6705 \pm 0.012	0.0365 \pm 0.020
LLM-Enhanced Methods						
LMD [24]	0.2011 \pm 0.012	0.4328 \pm 0.010	0.2774 \pm 0.045	0.2108 \pm 0.031	0.6356 \pm 0.015	0.0368 \pm 0.013
LLM-Blueprint [15]	0.1901 \pm 0.010	0.4561 \pm 0.013	0.2705 \pm 0.012	0.1943 \pm 0.011	0.6513 \pm 0.011	0.0312 \pm 0.010
Ranni [12]	0.1897 \pm 0.011	0.4289 \pm 0.011	0.2619 \pm 0.022	0.2002 \pm 0.012	0.6568 \pm 0.010	0.0313 \pm 0.021
Ours (RAVEL)						
Flux + Ours	0.3311 \pm 0.017	0.6810 \pm 0.033	0.5824 \pm 0.028	0.4220 \pm 0.024	0.2881 \pm 0.019	0.0867 \pm 0.010
SDXL + Ours	0.3011 \pm 0.016	0.6856 \pm 0.032	0.5691 \pm 0.027	0.4115 \pm 0.022	0.3225 \pm 0.020	0.0752 \pm 0.009
DALL-E + Ours	0.3356 \pm 0.018	0.7456 \pm 0.035	0.6421 \pm 0.029	0.4478 \pm 0.026	0.2661 \pm 0.017	0.0932 \pm 0.010

prompt-to-image alignment metrics less informative. To address this, we compute text-image alignment metrics such as CLIP-T and SigLIP by comparing the text embeddings of a character’s ground-truth contextual description with the embeddings of the generated image. This provides deeper insight into how well the generated images reflect the expected characteristics of rare entities. Similarly, we assess image-image alignment using CLIP-I, DINO v2, and LPIPS by comparing generated images against reference images from authoritative sources.

To further enrich our evaluation, we leverage the BLIP-VQA model to generate structured descriptions of key aspects of the generated images - such as appearance traits, background, and accessories. We then measure the semantic similarity between these descriptions and the ground-truth context, yielding BLIP scores that offer an additional layer of alignment assessment. This approach is applied to both baseline model outputs and images generated using our method. Our findings indicate a substantial improvement in both text-image and image-image alignment metrics, demonstrating that our approach effectively grounds image generation in precise, character-specific contexts, mitigating the ambiguity inherent in traditional T2I models. Furthermore, RAVEL outperforms other RAG-based and LLM-enhanced methods as shown in the Table. 2. This could be attributed to the fact that unlike these methods, our approach works even in the absence of visual priors. Also, KG-based RAG provides significantly superior and complete attribute retrieval, enhancing the quality of prompts for the T2I generation. Structured attribute retrieval ensures tight attribute

clustering & coverage, demonstrating the benefits of our graph-driven relational guidance, even in data sparse and complex concept structure scenarios.

This trend of improvement in metrics extends to self-correction, as shown in Table 3, where our SRD algorithm iteratively improves contextual alignment with each cycle of refinement, taking less time compared to SOTA methods. Repetitive generation and averaging of metrics using random resampling, and other self-correction methods still depend on the models’ pretrained knowledge, hence failing for cases when the model is not trained on those images or visual priors are absent. Furthermore, our approach significantly improves the ability of ControlNet to perform contextually accurate and narratively rich edits by incorporating relational details of rare characters as seen in Table 4. While other metrics show similar trends, note that the LPIPS metric represents an inherent trade-off when it comes to editing. While we want to lower LPIPS to enhance perceptual similarity of the edited images with the ground truth images, we also want to ensure meaningful modifications to the image due to editing, hence increasing LPIPS. Our approach carefully balances this trade-off. While RAVEL’s CLIP-I, CLIP-T remain higher and LPIPS lower for image generation across CLIP-LPIPS plots, our method successfully takes up the upper-left corner for editing, achieving high CLIP similarity scores and balanced LPIPS scores.

Since conventional metrics may struggle to capture nuanced and context-sensitive details essential to distinguish complex attributes in rare characters, we further integrate the ‘LLM as a Judge’ [55] framework. This

Table 3. **Self-Correction Performance Comparison.** RAVEL with SRD outperforms prior baselines in accuracy, alignment, and efficiency.

Method	Rounds	CLIP-T \uparrow	CLIP-I \uparrow	DINO \uparrow	BLIP-VQA \uparrow	LPIPS \downarrow	SigLIP \uparrow	Time (s) \downarrow
Base Models (no correction)								
Flux	0	0.1871 \pm 0.012	0.418 \pm 0.0018	0.2871 \pm 0.019	0.2278 \pm 0.018	0.5802 \pm 0.031	0.0634 \pm 0.007	62.5
SDXL	0	0.1842 \pm 0.013	0.297 \pm 0.0013	0.2619 \pm 0.017	0.1994 \pm 0.016	0.6234 \pm 0.034	0.0335 \pm 0.005	8.3
DALL-E 3	0	0.2201 \pm 0.014	0.4802 \pm 0.027	0.3667 \pm 0.022	0.2789 \pm 0.020	0.5677 \pm 0.030	0.0689 \pm 0.008	34.2
Test-Time Scaling (random resampling)								
Flux + Resample (N=4)	-	0.1908 \pm 0.003	0.4121 \pm 0.014	0.2278 \pm 0.013	0.2281 \pm 0.012	0.5640 \pm 0.012	0.0568 \pm 0.003	245.8
Flux + Resample (N=8)	-	0.1893 \pm 0.002	0.4050 \pm 0.012	0.2787 \pm 0.010	0.2127 \pm 0.001	0.5521 \pm 0.014	0.0562 \pm 0.004	493.6
Other Self-Correction Methods								
SLD [48]	2-3	0.2510 \pm 0.010	0.4822 \pm 0.022	0.3561 \pm 0.019	0.2891 \pm 0.021	0.5711 \pm 0.026	0.0623 \pm 0.004	178.7
ReflectionFlow [56]	16	0.2472 \pm 0.005	0.5219 \pm 0.013	0.3891 \pm 0.011	0.3127 \pm 0.015	0.5234 \pm 0.010	0.0781 \pm 0.005	312.3
RAVEL with SRD (Ours)								
Flux + SRD R1	1	0.3381 \pm 0.014	0.7110 \pm 0.032	0.6124 \pm 0.008	0.4320 \pm 0.014	0.2881 \pm 0.019	0.0962 \pm 0.021	155.5
Flux + SRD R2	2	0.3379 \pm 0.015	0.7515 \pm 0.030	0.6412 \pm 0.026	0.4413 \pm 0.023	0.2945 \pm 0.018	0.1302 \pm 0.012	267.8
SDXL + SRD R1	1	0.3121 \pm 0.011	0.7156 \pm 0.012	0.5811 \pm 0.021	0.4215 \pm 0.022	0.3255 \pm 0.010	0.0912 \pm 0.009	46.2
SDXL + SRD R2	2	0.3205 \pm 0.014	0.7334 \pm 0.031	0.5978 \pm 0.025	0.4278 \pm 0.021	0.3301 \pm 0.011	0.1087 \pm 0.011	88.3
DALL-E 3 + SRD R1	1	0.3451 \pm 0.011	0.7512 \pm 0.015	0.6521 \pm 0.020	0.4518 \pm 0.022	0.2682 \pm 0.010	0.1021 \pm 0.010	75.9
DALL-E 3 + SRD R2	2	0.3678 \pm 0.016	0.7801 \pm 0.033	0.6933 \pm 0.028	0.4821 \pm 0.025	0.2787 \pm 0.016	0.1388 \pm 0.013	158.1

framework, which has demonstrated near-human reasoning capabilities, enables dynamic evaluation of generated images based on the narrative context retrieved from our knowledge graph. We sample 100 rare image prompts for each of the four benchmarks and evaluate them using the four metrics that we curate: Attribute Accuracy, Context Relevance, Visual Fidelity, and Intent Representation. The LLM Judge is tasked with assigning a score between 0 and 1 for each metric, ranging from poor to good, to evaluate the quality of the image based on these criteria. Overall Alignment is calculated using the weighted scores of the metrics with [0.6, 0.15, 0.1, 0.15] weights for the corresponding metrics to prioritize accurate character depictions without compromising visual quality and narrative coherence. Table 1 shows that our method significantly enhances context-aware character depiction across all baseline models and benchmarks, achieving an average improvement of over **30%** in attribute accuracy and overall alignment.

User Study: We conducted a controlled prolific.com user study (N=60) evaluating Attribute Accuracy, Visual Fidelity, Contextual Relevance, and Intent Representation across 100 generated images. Across 25 judgment tasks per participant, 91.93% of choices preferred RAVEL-enhanced outputs.

5. Ablation Studies

To evaluate each component in our framework, we conduct comprehensive ablation studies on a sample of 100 images across image generation, self-correction, and editing. We evaluate how the four contextually aware alignment metrics - Attribute Accuracy, Context Relevance, Visual Fidelity, and Intent Representation defined using the LLM-

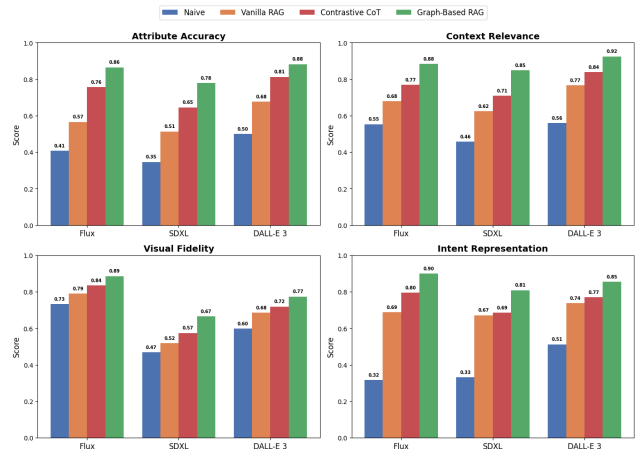


Figure 5. Ablation study demonstrating how different retrieval and prompting strategies contribute to RAVEL’s effectiveness in enhancing T2I models.

Judge framework vary with retrieval, prompting strategies.

Image Generation: We compare vanilla RAG, Contrastive CoT prompting, and our graph-based retrieval across Flux, SDXL, and DALL-E (Figure 5). All methods improve generation quality, with vanilla RAG boosting Flux’s attribute accuracy by 15% and intent representation by 35%. Contrastive CoT further enhances all four metrics by structuring multi-faceted context. Our graph-based retrieval outperforms both by providing rich, interconnected context that aligns images with both explicit and implicit attributes, yielding the highest gains across all models and metrics.

Self-Correction and Editing: We evaluate our SRD self-correction algorithm over two refinement iterations across four metrics and multiple T2I models. Each iteration yields

Table 4. Image editing performance comparison of ControlNet with and without our method. *We want to lower LPIPS as we are performing disentangled edits but not too low because we want to meaningfully modify the image so a moderate value indicates good performance.

Method	CLIP-T \uparrow	CLIP-I \uparrow	DINO \uparrow	BLIP-VQA \uparrow	LPIPS \downarrow^*	SigLIP \uparrow
Instruction-Based Editing						
InstructPix2Pix [4]	0.2912 \pm 0.012	0.9014 \pm 0.018	0.8812 \pm 0.014	0.3685 \pm 0.011	0.0894 \pm 0.006	0.1011 \pm 0.008
Prompt2Prompt [19]	0.2756 \pm 0.010	0.9120 \pm 0.020	0.8898 \pm 0.015	0.3723 \pm 0.012	0.0825 \pm 0.005	0.0964 \pm 0.007
DiffEdit [8]	0.3033 \pm 0.011	0.9187 \pm 0.016	0.9021 \pm 0.013	0.3792 \pm 0.010	0.0762 \pm 0.004	0.1073 \pm 0.006
Model-Based						
ControlNet (base)	0.3179 \pm 0.011	0.9810 \pm 0.020	0.9392 \pm 0.001	0.3682 \pm 0.021	0.0638 \pm 0.010	0.1102 \pm 0.001
HIVE [53]	0.3015 \pm 0.013	0.9265 \pm 0.017	0.9110 \pm 0.012	0.3756 \pm 0.011	0.2313 \pm 0.004	0.1155 \pm 0.007
GenArtist [44]	0.3078 \pm 0.014	0.9342 \pm 0.018	0.9159 \pm 0.013	0.3768 \pm 0.012	0.2274 \pm 0.005	0.1183 \pm 0.006
ControlNet + RAVEL (Ours)	0.3578 \pm 0.021	0.9401 \pm 0.006	0.9221 \pm 0.022	0.4291 \pm 0.001	0.2835 \pm 0.002	0.1279 \pm 0.012

Table 5. **User Study Results.** Percentage of user preferences for each T2I model with and without RAVEL.

Model	Attr. Acc.	Vis. Fidelity	Context Rel.	Intent Repr.
Flux (baseline)	58.2%	60.1%	56.3%	55.0%
Flux + RAVEL	92.4%	90.3%	91.2%	89.7%
SDXL (baseline)	61.5%	63.8%	59.2%	57.9%
SDXL + RAVEL	90.1%	88.6%	90.4%	87.8%
DALL-E 3 (baseline)	60.3%	62.0%	58.1%	56.5%
DALL-E 3 + RAVEL	91.6%	89.4%	90.8%	88.9%

clear gains by progressively strengthening weak or missing attributes through structured, context-aware prompt updates. Naïve baselines perform poorly due to their lack of contextual grounding, while our graph-based RAG initialization already provides strong improvements by supplying coherent, attribute-complete context. SRD further reduces hallucinations, sharpens attribute fidelity, and improves semantic alignment across models. For editing, standard ControlNet often introduces generic or misaligned modifications when applied to rare concepts. Integrating our method yields context-aware edits that preserve core attributes, substantially improving performance on all four evaluation metrics.

6. Conclusion

We present RAVEL, a graph-based RAG framework that enhances T2I diffusion models by addressing limitations in representing rare, domain-specific concepts. By leveraging structured knowledge graphs, RAVEL improves accuracy, consistency, and cultural alignment without requiring fine-tuning. It supports context-aware editing and iterative self-correction, enabling faithful generations and advanced relational modifications. Compatible with models like SDXL, Flux, and ControlNet, RAVEL offers a versatile solution for controllable, knowledge-grounded image generation.

References

- [1] Amazon Web Services, Inc. Improve your stable diffusion prompts with retrieval-augmented generation, 2023. Accessed: November 15, 2024. [2](#)
- [2] Patrice B  chard and Orlando Marquez Ayala. Reducing hallucination in structured outputs via retrieval-augmented generation. *arXiv preprint arXiv:2404.08189*, 2024. [2](#)
- [3] Andreas Blattmann, Robin Rombach, Kaan Oktay, Jonas M  ller, and Bj  rn Ommer. Retrieval-augmented diffusion models. In *Advances in Neural Information Processing Systems*, pages 20621–20637. Curran Associates, Inc., 2022. [2](#), [6](#), [7](#)
- [4] Tim Brooks, Aleksander Holynski, and Alexei A Efros. Instructpix2pix: Learning to follow image editing instructions. In *Proceedings of the IEEE/CVF conference on computer vision and pattern recognition*, pages 18392–18402, 2023. [3](#), [9](#)
- [5] Tom Brown, Benjamin Mann, Nick Ryder, Melanie Subbiah, Jared D Kaplan, Prafulla Dhariwal, Arvind Neelakantan, Pranav Shyam, Girish Sastry, Amanda Askell, et al. Language models are few-shot learners. *Advances in neural information processing systems*, 33:1877–1901, 2020. [2](#), [3](#)
- [6] Wenhui Chen, Hexiang Hu, Chitwan Saharia, and William W Cohen. Re-imagen: Retrieval-augmented text-to-image generator. *arXiv preprint arXiv:2209.14491*, 2022. [2](#)
- [7] Yew Ken Chia, Guizhen Chen, Luu Anh Tuan, Soujanya Poria, and Lidong Bing. Contrastive chain-of-thought prompting. *arXiv preprint arXiv:2311.09277*, 2023. [2](#), [3](#)
- [8] Guillaume Couairon, Jakob Verbeek, Holger Schwenk, and Matthieu Cord. Diffedit: Diffusion-based semantic image editing with mask guidance. *arXiv preprint arXiv:2210.11427*, 2022. [3](#), [9](#)
- [9] DeepEval Developers. DeepEval: The llm evaluation framework, 2024. [4](#)
- [10] Patrick Esser, Sumith Kulal, Andreas Blattmann, Rahim Entezari, Jonas M  ller, Harry Saini, Yam Levi, Dominik Lorenz, Axel Sauer, Frederic Boesel, et al. Scaling rectified flow transformers for high-resolution image synthesis. In *Forty-first international conference on machine learning*, 2024. [2](#)
- [11] Weixi Feng, Wanrong Zhu, Tsu-jui Fu, Varun Jampani, Arjun Akula, Xuehai He, Sugato Basu, Xin Eric Wang, and William Yang Wang. Layoutgpt: Compositional visual planning and generation with large language models. *Advances in Neural Information Processing Systems*, 36:18225–18250, 2023. [2](#)
- [12] Yutong Feng, Biao Gong, Di Chen, Yujun Shen, Yu Liu, and Jingren Zhou. Ranni: Taming text-to-image diffusion for accurate instruction following. In *Proceedings of the IEEE/CVF Conference on Computer Vision and Pattern Recognition (CVPR)*, pages 4744–4753, 2024. [2](#), [6](#), [7](#)
- [13] Robert M French. Catastrophic forgetting in connectionist networks. *Trends in cognitive sciences*, 3(4):128–135, 1999. [2](#)
- [14] Rinon Gal, Yuval Alaluf, Yuval Atzmon, Or Patashnik, Amit H Bermano, Gal Chechik, and Daniel Cohen-Or. An image is worth one word: Personalizing text-to-image generation using textual inversion. *arXiv preprint arXiv:2208.01618*, 2022. [2](#)
- [15] Hanan Gani, Shariq Farooq Bhat, Muzammal Naseer, Salman Khan, and Peter Wonka. Llm blueprint: Enabling text-to-image generation with complex and detailed prompts. *arXiv preprint arXiv:2310.10640*, 2023. [2](#), [6](#), [7](#)
- [16] Sreyan Ghosh, Chandra Kiran Reddy Evuru, Sonal Kumar, Deepali Aneja, Zeyu Jin, Ramani Duraiswami, Dinesh Manocha, et al. A closer look at the limitations of instruction tuning. *arXiv preprint arXiv:2402.05119*, 2024. [2](#)
- [17] Filip Gralinski, Anna Wr  blewska, Tomasz Stanis  lawek, Kamil Grabowski, and Tomasz G  recki. Geval: Tool for debugging nlp datasets and models. In *Proceedings of the 2019 ACL workshop BlackboxNLP: analyzing and interpreting neural networks for NLP*, pages 254–262, 2019. [6](#)
- [18] Hang Guo, Tao Dai, Zhihao Ouyang, Taolin Zhang, Yaohua Zha, Bin Chen, and Shu-tao Xia. Refir: Grounding large restoration models with retrieval augmentation. *Advances in Neural Information Processing Systems*, 37:46593–46621, 2024. [2](#)
- [19] Amir Hertz, Ron Mokady, Jay Tenenbaum, Kfir Aberman, Yael Pritch, and Daniel Cohen-Or. Prompt-to-prompt image editing with cross attention control.(2022). *URL https://arxiv.org/abs/2208.01626*, 3, 2022. [3](#), [9](#)
- [20] Jonathan Ho, Ajay Jain, and Pieter Abbeel. Denoising diffusion probabilistic models. *Advances in neural information processing systems*, 33:6840–6851, 2020. [1](#)
- [21] Edward J Hu, Yelong Shen, Phillip Wallis, Zeyuan Allen-Zhu, Yuanzhi Li, Shean Wang, Lu Wang, and Weizhu Chen. Lora: Low-rank adaptation of large language models. *arXiv preprint arXiv:2106.09685*, 2021. [2](#)
- [22] Kaiyi Huang, Kaiyue Sun, Enze Xie, Zhenguo Li, and Xi-hui Liu. T2i-compbench: A comprehensive benchmark for open-world compositional text-to-image generation. In *Advances in Neural Information Processing Systems*, pages 78723–78747. Curran Associates, Inc., 2023. [4](#), [6](#)
- [23] Patrick Lewis, Ethan Perez, Aleksandra Piktus, Fabio Petroni, Vladimir Karpukhin, Naman Goyal, Heinrich K  ttler, Mike Lewis, Wen-tau Yih, Tim Rockt  schel, et al. Retrieval-augmented generation for knowledge-intensive nlp tasks. *Advances in neural information processing systems*, 33:9459–9474, 2020. [2](#)
- [24] Long Lian, Boyi Li, Adam Yala, and Trevor Darrell. Llm-grounded diffusion: Enhancing prompt understanding of text-to-image diffusion models with large language models. *arXiv preprint arXiv:2305.13655*, 2023. [2](#), [6](#), [7](#)
- [25] Vivian Liu and Lydia B Chilton. Design guidelines for prompt engineering text-to-image generative models. In *Proceedings of the 2022 CHI conference on human factors in computing systems*, pages 1–23, 2022. [1](#)
- [26] Yang Liu, Dan Iter, Yichong Xu, Shuohang Wang, Ruochen Xu, and Chenguang Zhu. G-eval: Nlg evaluation using gpt-4 with better human alignment. *arXiv preprint arXiv:2303.16634*, 2023. [4](#), [6](#)
- [27] Chen-Yi Lu, Shubham Agarwal, Md Mehrab Tanjim, Kanak Mahadik, Anup Rao, Subrata Mitra, Shiv Kumar Saini, Saurabh Bagchi, and Somali Chatterji. Recon: Training-free

- acceleration for text-to-image synthesis with retrieval of concept prompt trajectories. In *European Conference on Computer Vision*, pages 288–306. Springer, 2024. 2, 6, 7
- [28] Yuanhuiyi Lyu, Xu Zheng, Lutao Jiang, Yibo Yan, Xin Zou, Huiyu Zhou, Linfeng Zhang, and Xuming Hu. Realrag: Retrieval-augmented realistic image generation via self-reflective contrastive learning. *arXiv preprint arXiv:2502.00848*, 2025. 2
- [29] Neo4j Inc. Neo4j: The graph database platform, 2023. Accessed: November 14, 2024. 4
- [30] Alex Nichol, Prafulla Dhariwal, Aditya Ramesh, Pranav Shyam, Pamela Mishkin, Bob McGrew, Ilya Sutskever, and Mark Chen. Glide: Towards photorealistic image generation and editing with text-guided diffusion models. *arXiv preprint arXiv:2112.10741*, 2021. 1
- [31] OpenAI. DALL-E 3. <https://openai.com/index/dall-e-3/>, 2023. 2
- [32] Boci Peng, Yun Zhu, Yongchao Liu, Xiaohe Bo, Haizhou Shi, Chuntao Hong, Yan Zhang, and Siliang Tang. Graph retrieval-augmented generation: A survey. *arXiv preprint arXiv:2408.08921*, 2024. 2
- [33] Dustin Podell, Zion English, Kyle Lacey, Andreas Blattmann, Tim Dockhorn, Jonas Müller, Joe Penna, and Robin Rombach. Sdxl: Improving latent diffusion models for high-resolution image synthesis. *arXiv preprint arXiv:2307.01952*, 2023. 1
- [34] Robin Rombach, Andreas Blattmann, Dominik Lorenz, Patrick Esser, and Björn Ommer. High-resolution image synthesis with latent diffusion models. In *Proceedings of the IEEE/CVF conference on computer vision and pattern recognition*, pages 10684–10695, 2022. 2
- [35] Chitwan Saharia, William Chan, Saurabh Saxena, Lala Li, Jay Whang, Emily L Denton, Kamyar Ghasemipour, Raphael Gontijo Lopes, Burcu Karagol Ayan, Tim Salimans, et al. Photorealistic text-to-image diffusion models with deep language understanding. *Advances in neural information processing systems*, 35:36479–36494, 2022. 1
- [36] Dvir Samuel, Rami Ben-Ari, Simon Raviv, Nir Darshan, and Gal Chechik. Generating images of rare concepts using pre-trained diffusion models. In *Proceedings of the AAAI Conference on Artificial Intelligence*, pages 4695–4703, 2024. 1, 6, 7
- [37] Priyanka Sen, Sandeep Mavadia, and Amir Saffari. Knowledge graph-augmented language models for complex question answering. In *Proceedings of the 1st Workshop on Natural Language Reasoning and Structured Explanations (NLRSE)*, pages 1–8, 2023. 2
- [38] Rotem Shalev-Arkushin, Rinon Gal, Amit H Bermano, and Ohad Fried. Imagerag: Dynamic image retrieval for reference-guided image generation. *arXiv preprint arXiv:2502.09411*, 2025. 2, 6, 7
- [39] Robik Shrestha, Yang Zou, Qiuyu Chen, Zhiheng Li, Yusheng Xie, and Siqi Deng. Fairrag: Fair human generation via fair retrieval augmentation. In *Proceedings of the IEEE/CVF Conference on Computer Vision and Pattern Recognition*, pages 11996–12005, 2024. 2
- [40] Jiaming Song, Chenlin Meng, and Stefano Ermon. Denoising diffusion implicit models. *arXiv preprint arXiv:2010.02502*, 2020. 1
- [41] Haoran Tang, Jieren Deng, Zhihong Pan, Hao Tian, Pratik Chaudhari, and Xin Zhou. Retribooru: Leakage-free retrieval of conditions from reference images for subject-driven generation. 2024. 2
- [42] Hugo Touvron, Thibaut Lavril, Gautier Izacard, Xavier Martinet, Marie-Anne Lachaux, Timothée Lacroix, Baptiste Rozière, Naman Goyal, Eric Hambro, Faisal Azhar, et al. Llama: Open and efficient foundation language models. *arXiv preprint arXiv:2302.13971*, 2023. 2
- [43] Xuezhi Wang, Jason Wei, Dale Schuurmans, Quoc Le, Ed Chi, Sharan Narang, Aakanksha Chowdhery, and Denny Zhou. Self-consistency improves chain of thought reasoning in language models. *arXiv preprint arXiv:2203.11171*, 2022. 2
- [44] Zhenyu Wang, Aoxue Li, Zhenguo Li, and Xihui Liu. Genartist: Multimodal llm as an agent for unified image generation and editing. *Advances in Neural Information Processing Systems*, 37:128374–128395, 2024. 6, 9
- [45] Zijie J Wang, Evan Montoya, David Munechika, Haoyang Yang, Benjamin Hoover, and Duen Horng Chau. Diffusiondb: A large-scale prompt gallery dataset for text-to-image generative models. *arXiv preprint arXiv:2210.14896*, 2022. 1
- [46] Jason Wei, Xuezhi Wang, Dale Schuurmans, Maarten Bosma, Fei Xia, Ed Chi, Quoc V Le, Denny Zhou, et al. Chain-of-thought prompting elicits reasoning in large language models. *Advances in neural information processing systems*, 35:24824–24837, 2022. 2, 3
- [47] Sam Witteveen and Martin Andrews. Investigating prompt engineering in diffusion models. *arXiv preprint arXiv:2211.15462*, 2022. 1
- [48] Tsung-Han Wu, Long Lian, Joseph E Gonzalez, Boyi Li, and Trevor Darrell. Self-correcting llm-controlled diffusion models. In *Proceedings of the IEEE/CVF Conference on Computer Vision and Pattern Recognition*, pages 6327–6336, 2024. 2, 6, 8
- [49] Shin’ya Yamaguchi and Takuma Fukuda. On the limitation of diffusion models for synthesizing training datasets. *arXiv preprint arXiv:2311.13090*, 2023. 1
- [50] Junyi Yao, Yijiang Liu, Zhen Dong, Mingfei Guo, Helan Hu, Kurt Keutzer, Li Du, Daquan Zhou, and Shanghang Zhang. Promptcot: Align prompt distribution via adapted chain-of-thought. In *Proceedings of the IEEE/CVF conference on computer vision and pattern recognition*, pages 7027–7037, 2024. 2
- [51] Shunyu Yao, Dian Yu, Jeffrey Zhao, Izhak Shafran, Tom Griffiths, Yuan Cao, and Karthik Narasimhan. Tree of thoughts: Deliberate problem solving with large language models. *Advances in neural information processing systems*, 36:11809–11822, 2023. 2
- [52] Lvmin Zhang, Anyi Rao, and Maneesh Agrawala. Adding conditional control to text-to-image diffusion models. In *Proceedings of the IEEE/CVF international conference on computer vision*, pages 3836–3847, 2023. 2

- [53] Shu Zhang, Xinyi Yang, Yihao Feng, Can Qin, Chia-Chih Chen, Ning Yu, Zeyuan Chen, Huan Wang, Silvio Savarese, Stefano Ermon, Caiming Xiong, and Ran Xu. Hive: Harnessing human feedback for instructional visual editing. In *Proceedings of the IEEE/CVF Conference on Computer Vision and Pattern Recognition (CVPR)*, pages 9026–9036, 2024. [3](#), [6](#), [9](#)
- [54] Yue Zhang, Hongliang Fei, Dingcheng Li, and Ping Li. Promptgen: Automatically generate prompts using generative models. In *Findings of the Association for Computational Linguistics: NAACL 2022*, pages 30–37, 2022. [2](#)
- [55] Lianmin Zheng, Wei-Lin Chiang, Ying Sheng, Siyuan Zhuang, Zhanghao Wu, Yonghao Zhuang, Zi Lin, Zhuohan Li, Dacheng Li, Eric Xing, Hao Zhang, Joseph E. Gonzalez, and Ion Stoica. Judging LLM-as-a-judge with MT-bench and chatbot arena. In *Thirty-seventh Conference on Neural Information Processing Systems Datasets and Benchmarks Track*, 2023. [4](#), [7](#)
- [56] Le Zhuo, Liangbing Zhao, Sayak Paul, Yue Liao, Renrui Zhang, Yi Xin, Peng Gao, Mohamed Elhoseiny, and Hongsheng Li. From reflection to perfection: Scaling inference-time optimization for text-to-image diffusion models via reflection tuning. In *Proceedings of the IEEE/CVF International Conference on Computer Vision*, pages 15329–15339, 2025. [2](#), [6](#), [8](#)